

Highlighting cutting mechanisms encountered in carbon/epoxy composite drilling using orthogonal cutting

Y. Turki¹ · M. Habak² · R. Velasco² · P. Vantomme²

Received: 27 June 2016 / Accepted: 9 February 2017 / Published online: 3 March 2017
© Springer-Verlag London 2017

Abstract The current knowledge about composite material machining is inadequate for its optimum utilization in many applications owing to the complexity of the phenomena involved in the cutting area. The objective of this study is to investigate the cutting mechanisms during carbon/epoxy composite drilling. It has been found that fiber orientation relative to the cutting direction is a key factor affecting machining results. Orthogonal cutting has helped to understand phenomena involved in the cutting area. The most common mechanisms noted are shearing, bending, and fiber/matrix interface debonding. It has been also noticed that surface quality, temperature fields' cartographies, and cutting forces change markedly with fiber orientation.

Keywords Carbon/epoxy composite · Drilling · Orthogonal cutting · Damage · Cutting mechanism

✉ M. Habak
malek.habak@u-picardie.fr

Y. Turki
yosra.turki@hotmail.fr

R. Velasco
raphael.velasco@u-picardie.fr

P. Vantomme
pascal.vantomme@u-picardie.fr

¹ Laboratory of Applied Fluid Mechanics, Environment and Process Engineering, National School of Engineers of Sfax, Route Soukra Km 3.5, 3035 Sfax, Tunisia

² Laboratory of Innovative Technology, IUT of Amiens, GMP Department, University of Picardie Jules Verne, Avenue des Facultés Le Bailly, 80001 Amiens Cedex 1, France

1 Introduction

The aircraft industry is a sector of high complexity for both the techniques and the materials used. The current economic and ecological context requires constant innovations to improve efficiency. Weight reduction is a major issue in order to limit the operating costs; hence, the carbon fiber composites integrated to the structure parts, while maintaining good mechanical properties. The use of these materials adds new challenges during shaping as the material removal mechanisms cause several damages. The most common defects are delamination, fiber buckling, decohesion, and thermal degradation.

The most frequent machining process used is drilling. It is a needed operation to put together different parts of a structure. Delamination, which is a key parameter to assess damage in composite drilling [1, 2], can be observed using non-destructive methods. The factor commonly used to quantify delamination is the delamination factor F_d . It is the ratio between the nominal hole diameter and the maximum damaged diameter, and it does not take the damaged area into account [3–5]. Recently, Babu et al. [6, 7] set up an overview on delamination assessment methods.

Comparative studies of composite drilling have been conducted using various cutting conditions [8–10]. They have shown that the feed has a greater influence on the thrust force and the delamination than the spindle speed [11–14]. In fact, higher feed produces a higher energy applied to layers below the tool and hence substantially increases the thrust force F_z and the delamination factor [3, 5, 14, 15].

Moreover, delamination occurrence depends on the F_z value. The thrust force must be reduced and kept below a critical force corresponding to the delamination onset [16, 17]. Indeed, when this critical force is reached, a small bulge appears near the drilling axis. This causes delamination, which propagates due to high stress on the layers [18, 19]. This

damage is more pronounced at the hole exit than at its entrance [20, 21]. The critical thrust force depends on the tool geometry which defines the force distribution on the composite to drill [22–25]. Also, the tool wear behavior is correlated to F_z and delamination. Its size and thrust force increase with tool wear rising [2, 26]. So, it is of great importance to select appropriate tool geometries and to control this wear to minimize delamination [2, 9, 27].

When studying the effect of lay-up configuration on surface integrity during drilling CFRP composites, it has been proved that 135° ply presents the more damaged surface [28]. Earlier works have proven also that during carbon/epoxy composite drilling, the direction of the cutting speed compared to the fiber direction is of considerable importance on defect onset and location [29–32]. This angle changes continuously during a half-revolution of the cutting edge [27]. Bonnet [15] has found that defects at hole entrance and exit have been located in common areas (fibers positively oriented relatively to the cutting direction), but with a larger extent at the hole exit. Inside the hole, damaged areas appear when fibers are negatively oriented relative to the cutting direction. In addition, according to Gohorianu [33], the damage is observed twice at the hole entrance because of the fiber orientation symmetry relative to the hole center [31–33]. These damaged areas are visible between 135° and 45°, and their extent decreases with the feed decreasing. Moreover, it has been noted that defects are due to compression and bending in the interval [135°, 90°]. Between 90° and 45°, they are generated by tensile and bending [33].

Other studies have noted the presence of circularity and dimensional defects [15, 33]. The composite is an anisotropic material. Tool feed generates fibers tightening on the lists. This phenomenon depends on the cutting angle. According to Bonnet [15], the most sensitive angular position to fiber spring-back is 90°. After drilling, an irregular shape of the hole is observed with a diameter smaller than the drill diameter [15, 33]. Feed has also a great influence on the hole diameter which is close to the nominal one at high feed and high speed drilling and is larger than the nominal diameter at lower feed [34].

To better understand mechanisms that occur during drilling, orthogonal cutting is the most simplified and studied process [35–39]. Studies on orthogonal cutting of carbon composites have shown that several parameters have an influence on the cutting forces and the resulting composite workpiece.

Fiber orientation influences chip formation mechanisms [40]. Generally, the chip is separated from the material in the fiber direction, and fiber break occurs perpendicularly to its axis [35, 41, 42]. Several fiber failure modes have been identified [38, 39, 43, 44]. At an angle of 0° between fibers and cutting direction, chip formation is initialized at the contact cutting edge/composite and is propagated along the fiber/

matrix interface. Bending stresses are accumulated in the fibers. The chip breakout occurs ahead of the cutting tool when these stresses exceed the fiber failure stress.

When the fiber orientation increases up to 90°, the tool pushes the fibers toward the material located behind them, hence producing a slightly marked bending. In addition, the tool also induces a force in the fiber direction. This force makes the fibers easier to break near the cutting area. The compression generates fiber shearing.

The 90° orientation is a threshold, beyond which surface roughness is high. Indeed, fibers are perpendicular to the cutting direction. Chip formation is initiated along the fiber/matrix interface because of high interlaminar shear stresses. Reinforcement is bent forward as packets. Fracture perpendicular to the fibers is induced by compression, out of the cutting plane, and the extent of sub-surface defects is high. Indeed, 90° cutting generates fiber/matrix interfacial failure as sub-surface damage.

At 135°, the tool causes fiber bending and compression. During machining, the cutting edge lifts the fibers under the cutting force action, which leads to fiber/matrix interface debonding. The peeled fibers and the interfacial debonding generate bending stresses in the sub-surface, thereby producing fiber pullout.

The cutting process results in two forces: cutting and thrust forces. Experimental studies of orthogonal cutting mechanisms, performed on unidirectional composites, show that the following:

- The cutting force increases gradually until θ reaches 75° then raises suddenly at $\theta = 90^\circ$. The thrust force increases until θ is equal to 15°, and it remains almost constant until θ reaches 75° [43]. Bhatnagar et al. [41] highlight a contradiction, as they conclude that the thrust force decreases as θ goes from 0° to 75°.
- Cutting depth a_p has also a strong influence on the forces. The cutting and thrust forces rise linearly as a function of a_p [43, 45, 46]. Precisely, when a_p goes from 0.1 to 0.2 mm, the cutting force increases by 29% [46]. They have confirmed numerically these results by running a three-dimensional macromechanical finite element model.
- Iliescu [47] has indicated that the cutting speed V_c has nearly no influence on the cutting forces (V_c varied from 6 to 60 m min⁻¹). Wang et al. [43] have studied a range of lower cutting speeds (4, 9, and 14 m min⁻¹) and have observed the same result.
- When machining fibers with orientations up to 90°, the clearance angle has a strong influence on F_p rather than the rake angle [40]. For example, at the 30° orientation, a 20° increase of the rake angle leads to a feed force reduction of 5%. However, this force decreases by about 20% when the clearance angle increases by 14°.

The following study is focused on the drilling process of a carbon fiber-reinforced composite. The objective is to analyze the influence of layer orientation on the hole quality and cutting mechanisms. In order to assess these mechanisms and to understand the machinability of the composite, unidirectional laminates have been subjected to orthogonal cutting. This simple process will help understand the relations among fiber orientation and surface integrity and establish possible links between orthogonal cutting results and drilling results.

2 Damage and defects in a drilled composite

In the drilling investigation, Quasi-Isotropic QI carbon fiber-reinforced composites with a thickness of 7 mm and a stacking sequence of laminates of $[(0^\circ/45^\circ/90^\circ/135^\circ)_3]_s$ (24 layers) have been used. A mixture of SICOMIN thermoset epoxy resin and hardener has been implemented by infusion. The fiber rate, determined by pyrolysis, is 71.86%, with a standard deviation estimated to be 0.24%.

Drilling operations have been conducted on a milling machine under dry cutting conditions. A fixture including 10-mm-diameter holes has been firmly held on top of the dynamometer, to ensure a free drilling and no vibration. The drilling setup is shown in Fig. 1.

Tests have been conducted with an uncoated carbide twist drill (6 mm diameter). It has been largely identified in literature [11–13] that feed has a greater influence on delamination than spindle speed N . Tests have then been carried out at $N = 6000$ rpm using five different feeds ($f = 0.04, 0.1, 0.2, 0.3, \text{ and } 0.36$ mm/rev). Three holes have been made at each feed. Measurements of thrust force F_z and torque M_z have been performed using a Kistler dynamometer. After machining, macroscopic observations of the composite surfaces have been collected to quantify the feed effect on damages. The quality of the entrance, the inside, and the exit surfaces has been examined.

F_z increase is proportional to the feed (Table 1) as the thickness to drill per revolution increases as well. It can be noted that damage extension is correlated to F_z evolution, which has also been confirmed in literature [48–50].

The torque increases with the feed too (Table 1). It generates more defects and so uncut fibers which induces more friction on the tool and then a higher M_z , as noticed by [4]. It should be noted that the standard deviation is greater for the torque than for the thrust force.

Feed increase generates delamination and does not provide a straight cut. Indeed, a small feed ($f = 0.04$ mm/rev) results in minor defects at the hole entrance. Its increase causes damages which become visible to the naked eye. At high feeds, drilling favors peel up delamination and defects occupy a larger area. Damages observed are delamination, spalling, and uncut fibers that exceed the hole

periphery (Fig. 2). According to Bonnet et al. [27], when drilling with a 12-mm-diameter drill and a feed rate higher than 0.05 mm/rev, delamination exceeds the maximum damage ring of $\varnothing 14$ mm authorized by the aerospace industry.

Defects are also generated when the cutting edge is fully engaged in the hole. A destructive study of the holes illustrates that inside surfaces are strongly dependent of the fiber orientation (Fig. 2). Rough areas appear, characterized by pullout fibers, high delamination, and uncut fibers especially at high feeds. In fact, a high feed corresponds to a high linear extrusion speed, which in turn produces a high energy transmitted from the tool to the uncut layers [3], hence the occurrence of a more pronounced delamination, particularly at the free output folds. In order to reduce delamination, it is necessary to minimize thrust force and keep it below the critical stress corresponding to the delamination onset [16, 17, 22, 34].

Hole exit surfaces are marked with delaminated areas and uncut fibers, of different lengths and widths. It should be also noted that no trend has been identified as a function of the feed and that the defect shape and density have not been replicable. Indeed, uncut fibers have been observed whatever the cutting conditions and are hardly avoidable. In fact, the infusion manufacturing process generates a low adhesion of the fiber on the matrix on the mold side. Furthermore, when drilling with the twist drill, Rahme et al. [18] have highlighted the importance of the chisel edge. When it comes to the hole exit and the critical thrust force is reached, a small bulge appears near the drilling axis and then along the fiber direction and the surface tears. Thus, delamination is initiated and propagates due to continuous high stress on the layers [19]. Drilling without support promotes bending of the lower layers and does not impede their debonding at the hole exit. It should be noted that delamination at the hole exit is more severe than at the hole entrance, which has widely been proven [20, 21, 34], and that, once initiated at the hole entrance and exit, defects propagate along the fiber direction.

At the hole entrance, the damaged areas can be connected to particular fiber orientations relative to the cutting speed V_c direction. On the adopted scheme on Fig. 3, the colored area represents the damaged periphery while the colorless area corresponds to the straight cut fibers with no visible defect. As the drilling operation is not performed on a flat surface, the V_c direction is constantly changing relative to the fiber direction. And almost all the defects have been localized in the areas where the fibers are oriented at an angle χ equal or greater than 90° relative to the V_c direction (Fig. 3). These findings are in agreement with damage observations in [27].

Because of the fiber orientation symmetry relative to the hole center, the damage occurs twice on the hole periphery, which is in accordance with [27, 31, 32]. Figure 3 illustrates also that the defects extent depends on feed. At low feed, no

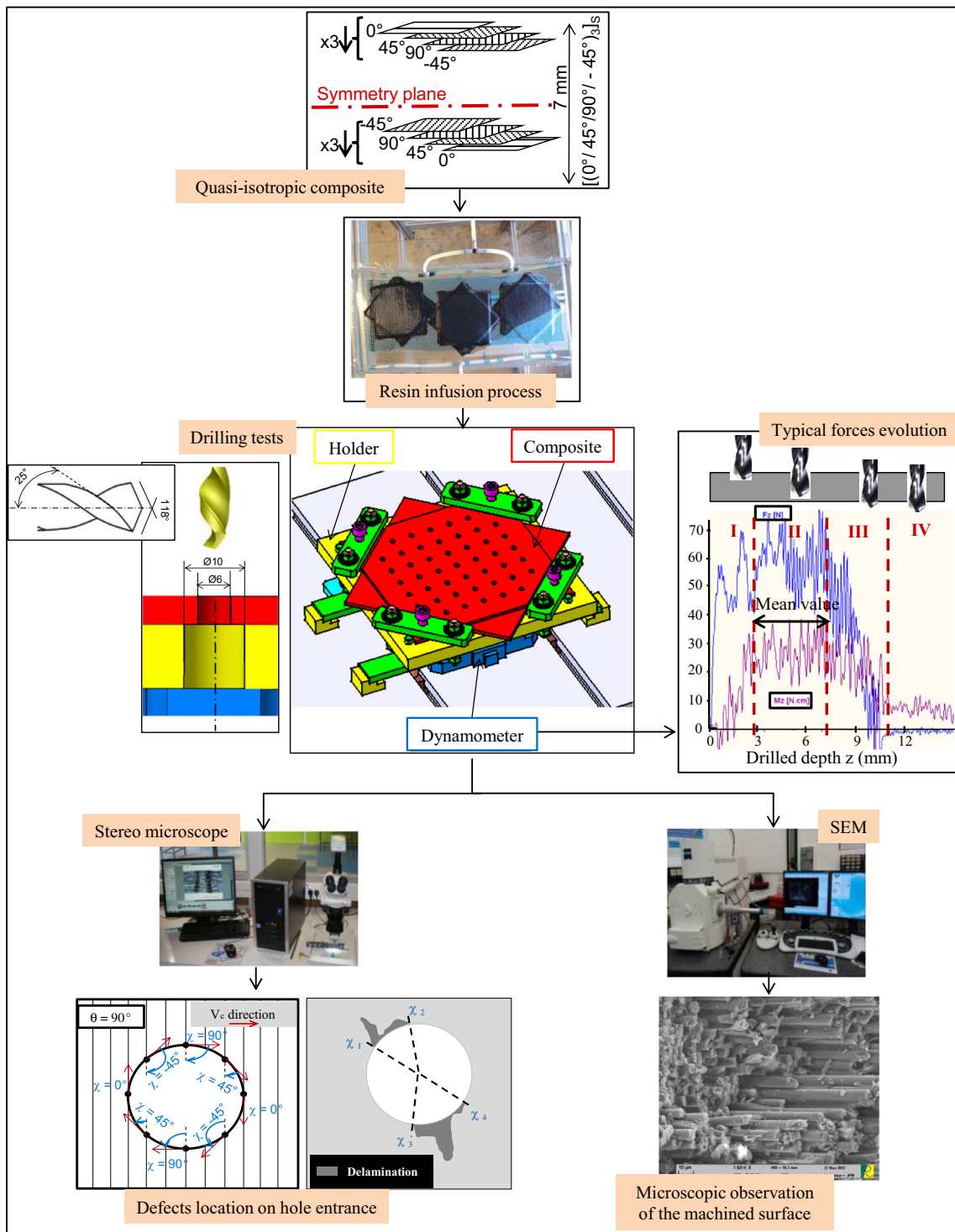


Fig. 1 Experimental drilling process setup

Table 1 Influence of feed on thrust force and torque (spindle speed $N = 6000$ rpm)

Feed f (mm/rev)	0.04	0.1	0.2	0.3	0.36
Thrust force F_z (N)	$41 \pm 4\%$	$48 \pm 4\%$	$66 \pm 4\%$	$72 \pm 4\%$	$77 \pm 4\%$
Torque M_z (N cm ⁻¹)	$11 \pm 13\%$	$17 \pm 13\%$	$23 \pm 13\%$	$36 \pm 13\%$	$38 \pm 13\%$

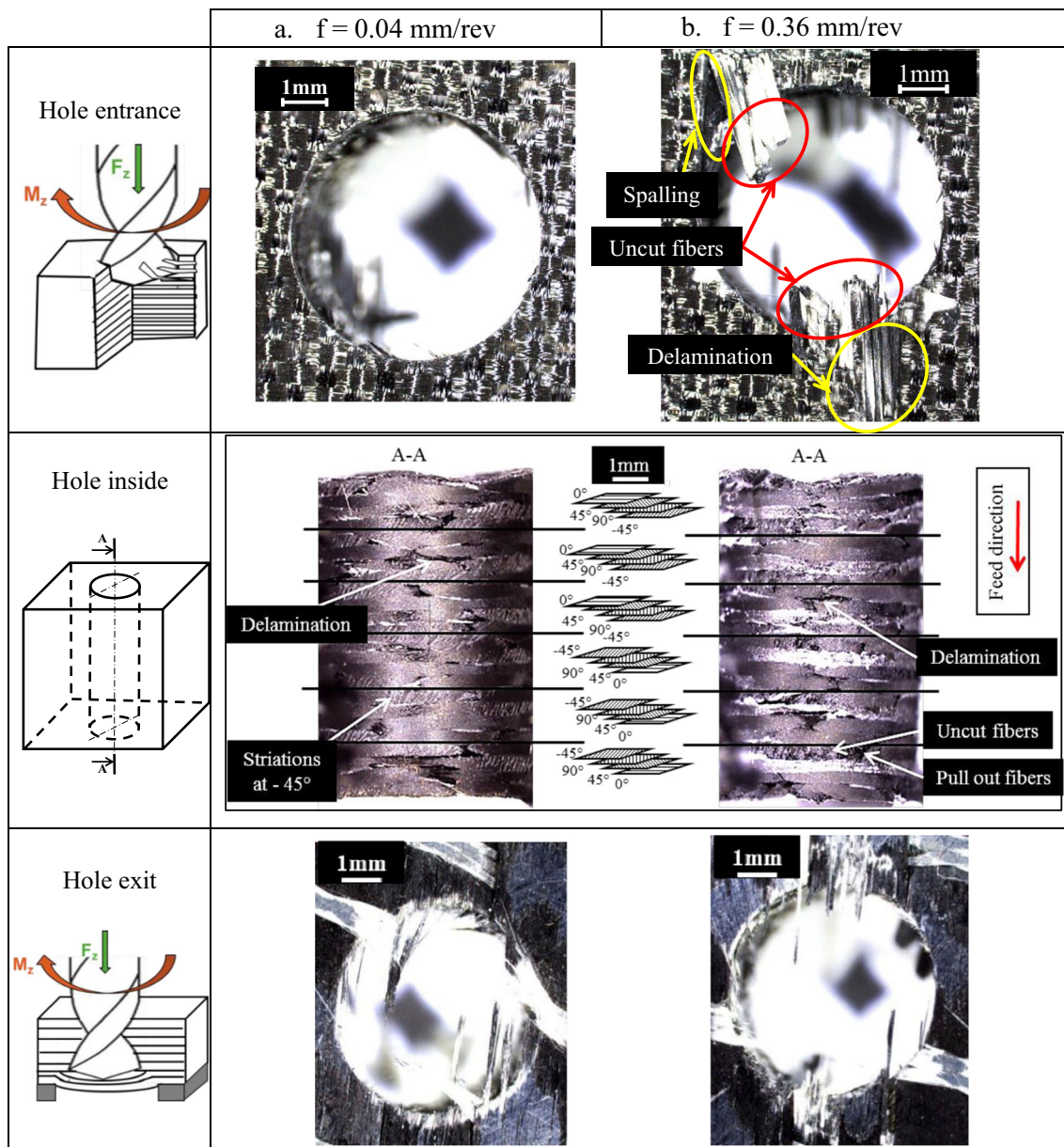


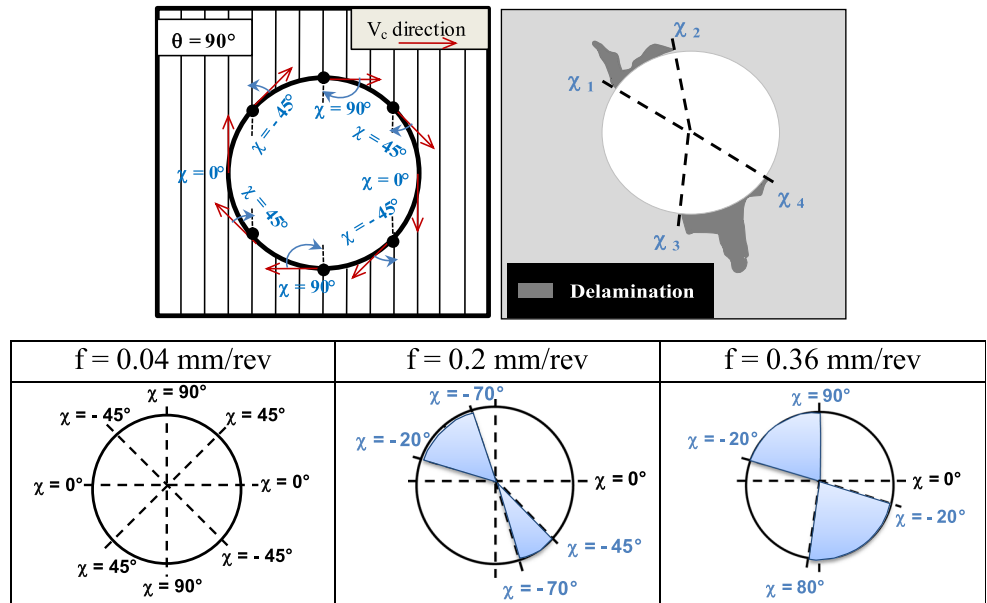
Fig. 2 Macroscopic observations of hole surfaces on a quasi-isotropic composite [51]

defect has been noticed on the hole entrance. The damaged area becomes then larger with the feed increase.

A non-destructive 3D tomography observation has allowed analyzing the inner layers. Figure 4 illustrates layers with various fiber orientations θ , relative to the manufacturing reference. Even in drilled depth, defects have been localized on the areas where the fibers are negatively oriented relative to the cutting speed direction. However, the damaged area is greatly reduced compared to the one at the hole entrance. Whatever the layer orientation, χ variation does not exceed the interval $[-30^\circ, -80^\circ]$. Indeed, each layer has been compacted by the other ones. The fibers are then better maintained and are less likely to be deformed under the cutting edge effect.

As mentioned, macroscopic observations have shown heterogeneous inside surfaces and the presence of significant defects. A microscopic analysis has then been carried out using a scanning electron microscope (SEM) to better understand the phenomena involved during cutting at the fiber scale. Figure 5 shows these microscopic observations for a stacking sequence of four layers $[0^\circ/45^\circ/90^\circ/135^\circ]$ of the QI composite. Surface quality changes from a layer to another. The best surface is noted at 0° relative to the cutting speed direction. At 45° , residues of broken fibers and molten resin are observed. At 90° , microscopic observation illustrates fiber/matrix debonding. The crack is initiated and propagates slowly until the fibers' breakout. The most damaged surface is observed at

Fig. 3 Defect location on the hole entrance with the feed f (spindle speed $N = 6000$ rpm)



135°. It is marked by pulled-out fibers. This is in accordance with Ramirez et al. [31]. They noted the maximal surface roughness at 135°.

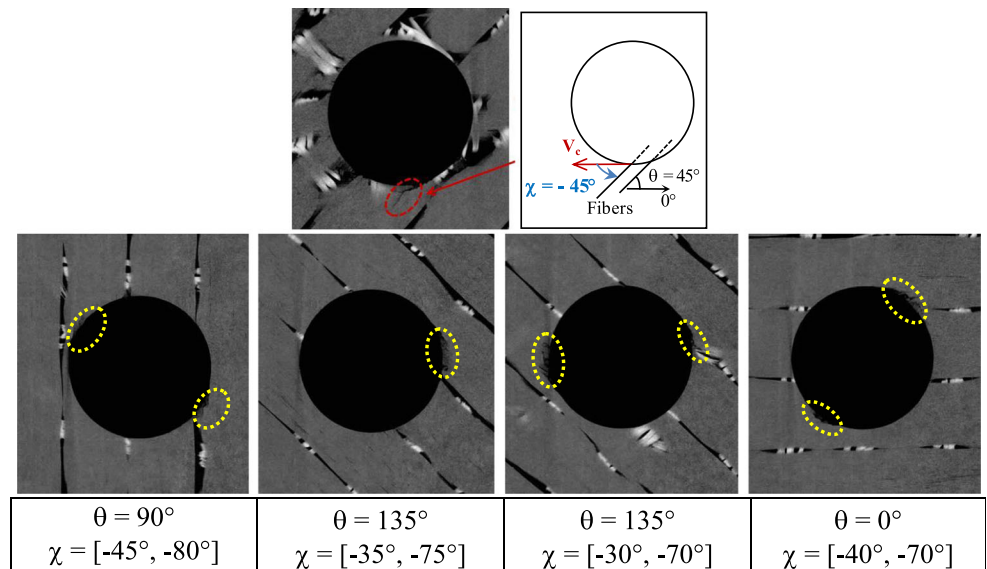
It has then been shown that defects on the drilled quasi-isotropic QI composite depend greatly on the fiber orientation and attention has been drawn to their location on very specific areas. As shown earlier, surface profiles at the hole entrance, inside, and exit are heterogeneous and several types of defects have been identified (decohesion, delamination, uncut and pulled-out fibers, cracks). To better understand the cutting mechanisms involved during drilling and responsible of the surfaces' quality, the cutting process has been simplified and orthogonal cutting has been investigated.

3 Analysis of chip formation mechanisms

Orthogonal cutting has been carried out on composite material to assess the cutting mechanisms responsible for the damage occurrence. Although this process is industrially a useless configuration, it is a necessary step to understand precisely the phenomena involved during cutting and to improve machining using more complex processes. A conventional configuration of the fiber orientation θ in the cutting zone has been established, which has been defined clockwise relative to the cutting direction. It therefore corresponds to the angle χ encountered in drilling.

Orthogonal cutting has been thus conducted on a unidirectional composite, and 15 layers have been stacked in

Fig. 4 3D tomography image of the inner layers (spindle speed $N = 6000$ rpm, feed $f = 0.36$ mm/rev)



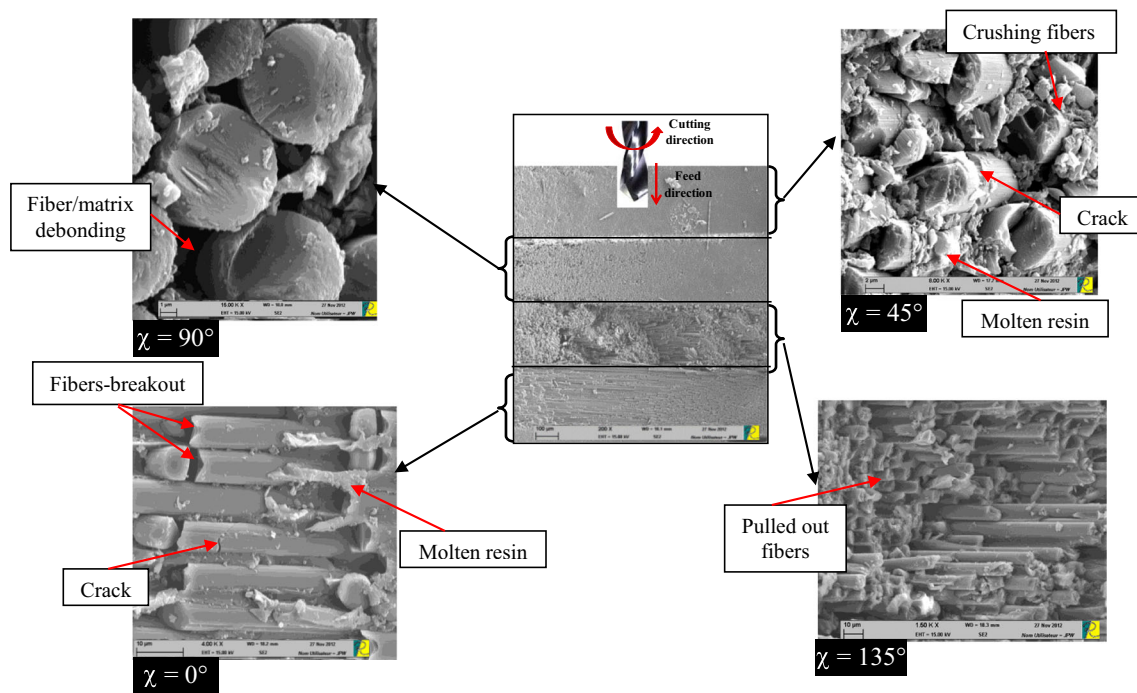


Fig. 5 Microscopic observation of four layers at the hole inside

the same direction. A length of 90 mm has been machined with several fiber orientations θ (0° , 15° , 30° , 45° , 60° , 90° , and 135°). An uncoated carbide tool designated by TCMW 16T304 has been used (Fig. 6). This insert, provided by T&O, is of grade KIC21 (ISO K05-K15). Rake angle γ and clearance angle α are equal to 0° and 7° , respectively. Tests have been performed at a cutting speed V_c of 28 m/min and a cutting depth a_p of 0.5 mm. The temperature fields, acquired at the cutting edge/material interface during machining, have been analyzed using a thermal imaging camera.

Microscopic observations have shown that surface and sub-surface damages are related to the fiber orientation (Fig. 7). Encountered cutting mechanisms are consistent with literature [8, 9, 12, 22].

- At 0° (Fig. 7a), fracture is introduced along the fiber/matrix interface by mode I (tensile opening) loading. Then during machining, mode II (in-plane shear) loading is observed. Finally, fiber fracture occurs perpendicularly to their direction under bending loads. Reinforcement is removed cleanly, due to fiber/matrix debonding. Minor damages are observed near the machined surface, and some sub-surface cracks are present perpendicularly to the fibers. At this orientation, the tool is in permanent contact with the material. The friction is high and the backflow is important. This behavior tends to generate high cutting temperatures ($T = 75^\circ\text{C}$) near the transition temperature of the epoxy resin.

- Cutting mechanisms are different when machining the other fiber orientations (Fig. 7b–d). In each case, the tool pushes the fibers toward the workpiece sub-surface. The material located behind the cut fibers prevents from a large bending. In the meantime, the thrust force generates a compressive stress to make the fiber easier to break near the cutting zone. As a result, when the θ value is lower than 90° , the combined forward and downward compressive tool load generates surfaces marked by crushed fibers. Material removal appears to be governed by the in-plane shear, and sub-surface damage is small.

Temperature fields' cartographies illustrate a chip's amount at 15° that rubs on the tool (Fig. 7b). At 45° , fibers' shearing is easy [38] and the chip is released in a spiral form. In this case, it rubs less than at 0° and 15° on the cutting edge. The temperature decreases between the orientations 0° and 45° ; it drops from 75 to 55°C .

- At 90° , the tool feed is perpendicular to the fiber orientation and fibers have a weaker support from the material located behind the cut fibers. After being pushed, fibers' bending is severe and the fracture of the epoxy resin is fast. In this case, fractures induced by a perpendicular compression of the fibers and fiber/matrix debonding are the cutting mechanisms involved. This leads to a rough surface and a deep sub-surface damage. Moreover, no backflow has been observed in front of the tool. Because of the fibers' high strength, the real depth of cut is lower

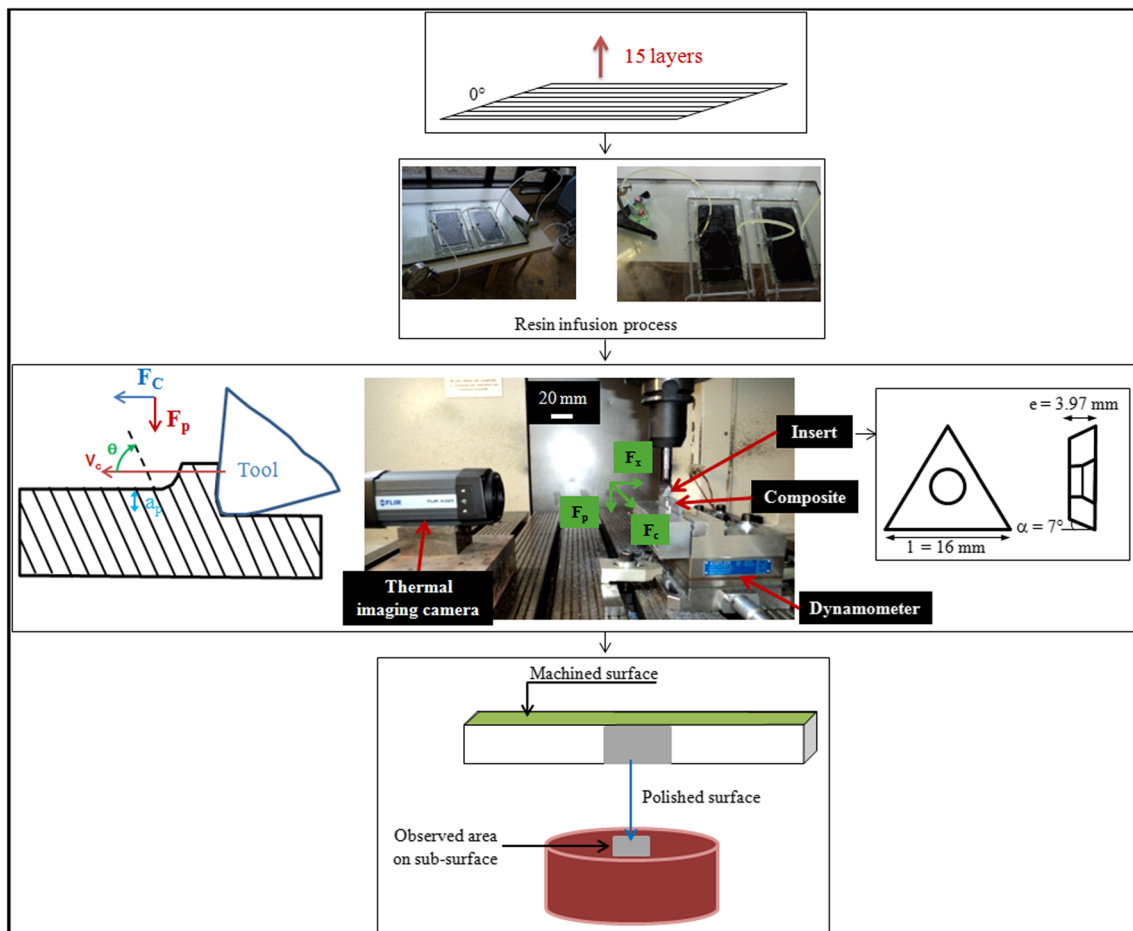


Fig. 6 Experimental orthogonal cutting process setup

than the nominal one and the chip is released in a dust form. Finally, less friction has been noted and Fig. 7e shows low temperature ($T = 35\text{ }^{\circ}\text{C}$).

- Beyond 90° , the tool pushes fibers which are in opposite direction of the tool feed. The fibers get less support from the surrounding materials. They are no longer maintained, and it is very difficult to shear them, leading to a more severe fiber bending and interlaminar fracture along the fiber/matrix interface. Out-of-plane displacement is noticed, and the fibers' fracture is due to severe macrodeformations induced by the compressive tool load. The quality of the surface becomes poor and the sub-surface is damaged, as cracks propagating in the depth and stair steps are encountered. These cutting mechanisms generate an increase of the material/tool contact area. The friction becomes significant at 135° , resulting in the highest cutting temperature noticed during the study, almost $90\text{ }^{\circ}\text{C}$.

It should be noted that, regardless of the fiber orientation, the highest temperature has been recorded and evacuated by the debris.

As already observed in Fig. 7, up to 90° , the damage's extent in the sub-surface, denoted as E_c , represents the cracks' length. At 135° , the profile has a shape of stairs and E_c corresponds to the height of the stair step. These extents are given in Fig. 8.

Values represent the average of all the damages observed microscopically along the sub-surface of the machined sample. As noticed in Fig. 7a–f, the lowest cracks' extent has been associated with the composite machined at 0° . From 15° to 60° , the cracks' propagation in the sub-surface decreases. A sudden increase has been observed at 90° with a high standard deviation between measurements. Indeed, E_c depends on the cracks' propagation in the fiber/matrix interface. For the orientation 90° , fiber breakage does not take place at the contact tool/material and the presence of pullout fibers is noted. Figure 8 has also shown that the greatest damage is observed at 135° , but with a low dispersion of the E_c values (standard deviation does not exceed 0.01 mm for an average E_c of 0.14 mm). These findings are in accordance with [40]. The 0° surface is very even with correctly oriented fibers despite being partly broken. Delamination does not occur. At 30° and 60° , similar surfaces are displayed, with lower bending fibers

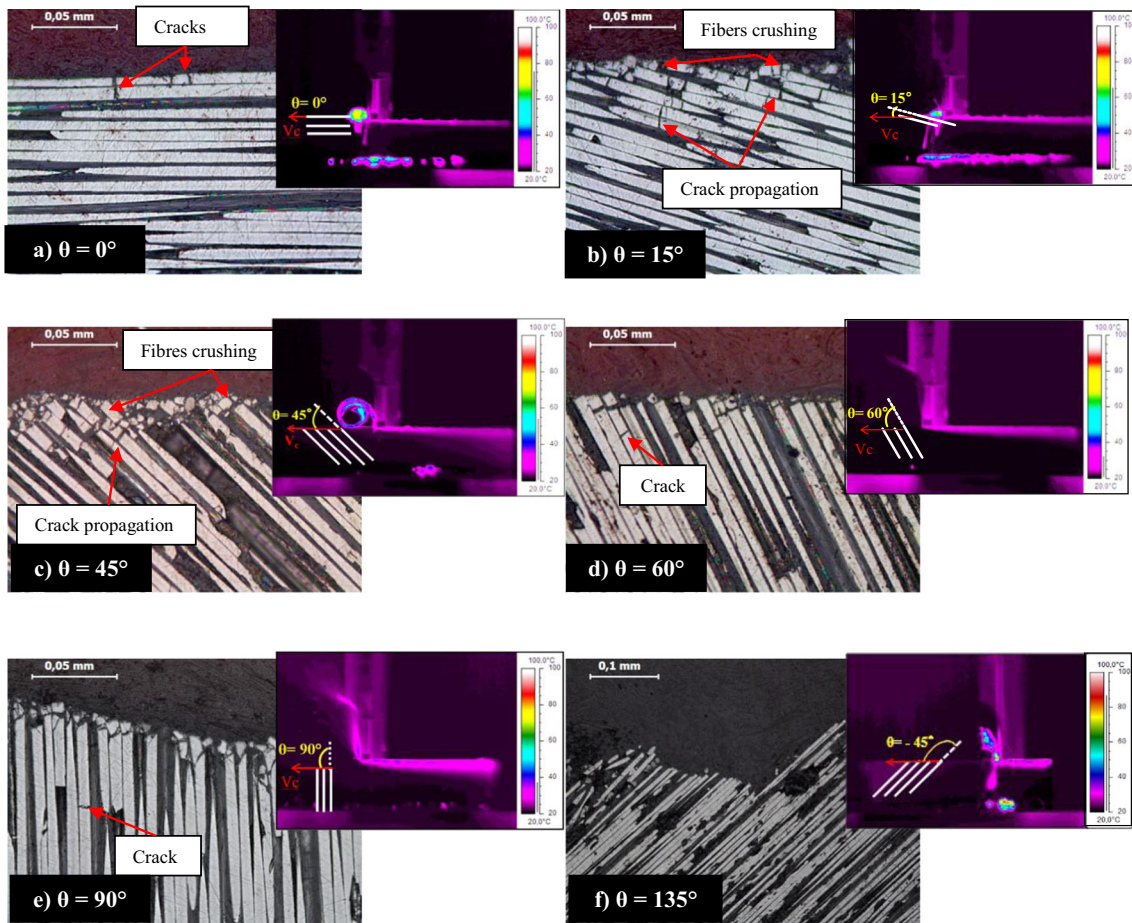
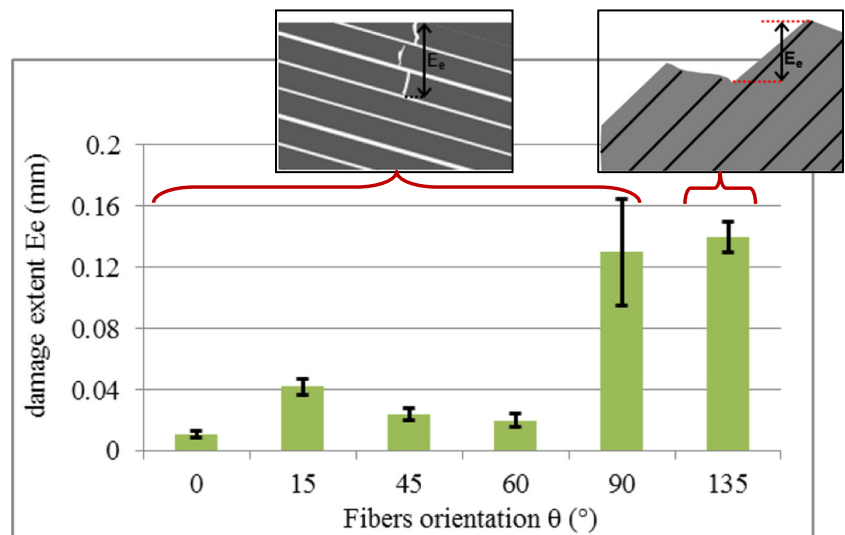


Fig. 7 Sub-surface microscopic observations and temperature field cartographies on orthogonal cutting (cutting speed $V_c = 28$ m/min, cutting depth $a_p = 0.5$ mm)

at 60°. The majority of fibers oriented at 90° are broken as far as 150 μ m underneath the surface. A high surface roughness was obtained at $\theta = 150^\circ$ with a saw tooth profile.

As for the chip formation, the fiber orientation θ is a key factor influencing the cutting forces. For convenience, forces along and perpendicular to the cutting direction are called the

Fig. 8 Evolution of sub-surface damage's extent as a function of fiber orientation



cutting force F_c and thrust force F_p , respectively. These forces depend on the fiber behavior during machining and can be related to microscopic observations (Fig. 9), which has been supposed by Henerichs et al. [40]. The interplay between CFRP fibers and flank face (friction, spring-back phenomenon, and amount of cut material diving under the cutting edge along the flank face) influences the thrust force evolution.

- At 0° , the depth to remove is separated from the UD composite by a fracture at the fiber/matrix interface. Moreover, the tool bends the fibers (lifted by mode I loading) under the cutting force effect. A high F_c has then been noticed. At 15° , the tool compresses the fibers which are substantially supported by the material located behind the cut fibers. These fibers apply a high force on the tool flank, and F_p is much greater at 15° cutting than at 0° . This explains the cracks' propagation over an extended distance on the sub-surface (Fig. 8).
- From 15° to 45° , fibers become more brittle and can be sheared and fractured easier. The thrust force and the sub-surface damage's extent decrease as observed in Fig. 8. A higher F_p at 30° rather than at 60° was also noted by Henerichs et al. [40] (they based their study on five orientations: 0° , 30° , 60° , 90° , and 150°). Indeed, bending has been more intense at 30° .

The cutting features in the cutting direction remain the same, and the cutting force is so nearly steady.

- From 45° to 90° , the cutting force increases. In fact, fiber strength in the direction perpendicular to the tool feed is substantial and a high stress is applied. At 90° , surface microscopic observations have illustrated fiber/matrix

debonding and pulled-out fibers (Fig. 9). Indeed, many fibers have been pushed, but not broken in the contact area. Figure 9 also shows that the thrust force is almost constant between 45° and 90° .

- When the fibers are negatively oriented ($\theta = 135^\circ$), the tool lifts them when progressing and the resin, which is fragile, is fractured quickly. The fibers are compressed and bent easily, and the cutting force and the thrust force are therefore lower than at the 90° orientation. These findings suit the conclusion drawn by Henerichs et al. [40]. They noted that the minor tool wear when machining fibers at 150° is in good agreement with the lowest feed forces. In addition, this orientation shows the lowest cutting force.

It should be also noted that the cutting force and the thrust force evolutions (Fig. 9) and the sub-surface assessment (Figs. 7 and 8) lead to a conclusion that forces and fiber orientation determine the machined surface quality. The relationship between these two factors depends on the support provided by the resin which surrounds the reinforcement and on the fiber strength. Between 15° and 45° , the material behind the pushed fibers is of importance. In this case, the influencing force is the thrust force and the cutting force is almost steady, as noted before. Beyond 45° , the epoxy resin is easily fractured. The machined surface becomes dependent on fiber strength to bending and to the stress applied by the tool in the cutting direction, whence on the cutting force.

A correlation between material removal mechanisms and defects observed in drilling and orthogonal cutting is proposed. The drilling-induced surface may, locally around the cutting zone, be divided into different areas observed in orthogonal cutting. Four chip formation's modes are identified, as shown in [31, 32].

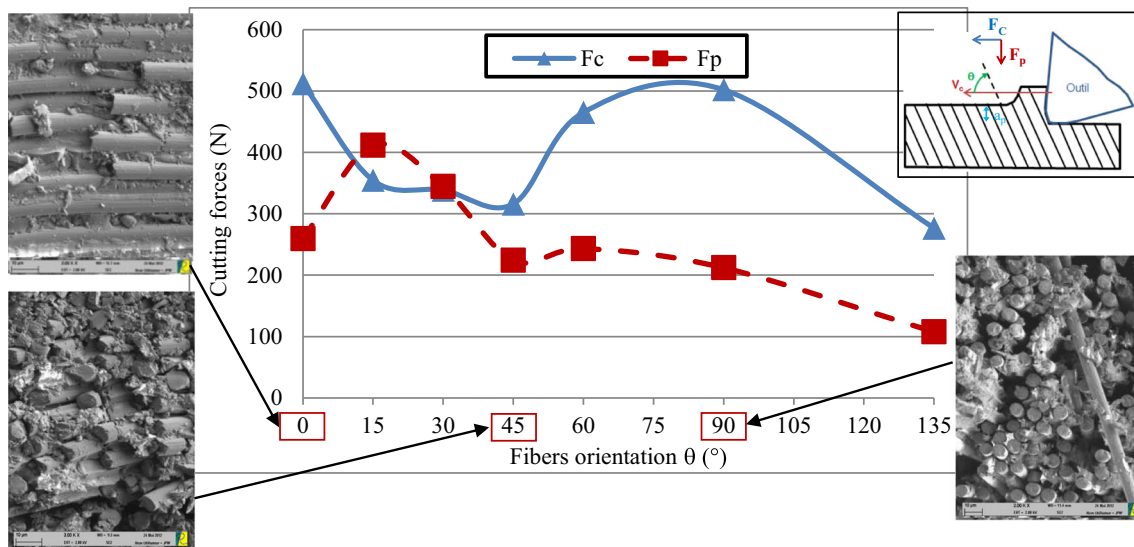


Fig. 9 Thrust force and cutting force evolution as a function of fiber orientation (cutting speed $V_c = 28$ m/min, cutting depth $a_p = 0.5$ mm)

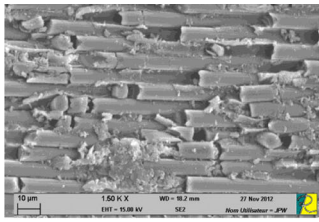
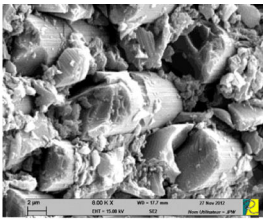
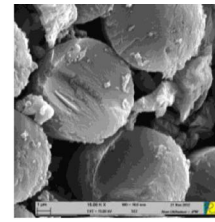
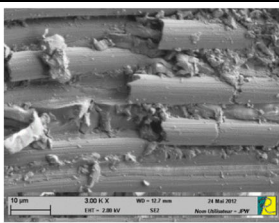
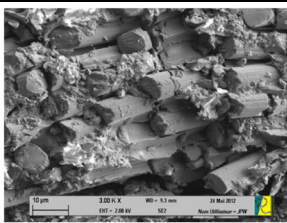
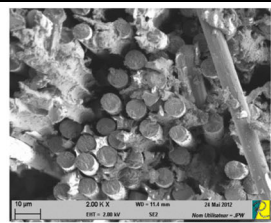
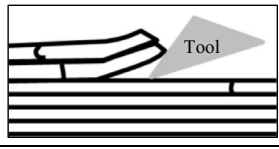
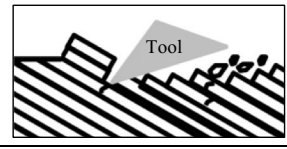
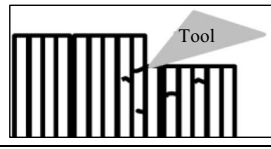
Drilling			
Fiber orientation	$\theta = 0^\circ$	$\theta = 45^\circ$	$\theta = 90^\circ$
Orthogonal cutting			
Cutting mechanisms			
	Delamination + Bending	Compression + Shearing	Fiber/matrix debonding + Shearing

Fig. 10 Chip formation mechanisms in drilling and orthogonal cutting

- *Mode 0°*: fibers are in the cutting direction. The crack is introduced and propagates at the fiber/matrix interface. The chip is formed by the fiber fracture under bending. The best surface quality is noticed (Fig. 10, $\theta = 0^\circ$).
- *Mode 45°*: fibers are easier to shear and fracture. Fiber fracture is due to compression, crushing, and shearing. Machined surfaces are marked by crushed fibers (Fig. 10, $\theta = 45^\circ$).
- *Mode 90°*: fibers are pushed during machining. The surfaces are marked by fiber/matrix debonding and pulled-out fibers. The fiber breakage consists of two phases: crack initiation perpendicularly to the fiber direction and sudden breakout (Fig. 10, $\theta = 90^\circ$).
- *Mode 135°*: fibers are submitted to a tensile stress and are strongly bent. Surface quality is the worst, and a stepped profile is observed after machining (Fig. 5, $\theta = 135^\circ$).

4 Conclusion

An experimental investigation has been performed to study the cutting mechanisms encountered in machining carbon/epoxy composites. Results show that fiber orientation relative to the cutting speed direction is a key factor which determines the surface quality in drilling.

Defects have been localized on the areas where fibers are oriented at an angle χ equal or greater than 90° , with larger extents at the hole entrance than at the inner layers. The most damaged areas have been noticed at the hole exit since an impregnation problem has been encountered and free drilling has been used.

Moreover, each area locally around the drilling zone corresponds to a surface obtained by orthogonal cutting. This simplified configuration achieves an understanding of the chip formation mechanisms of the carbon/epoxy composite. It helps also explain drilling-generated defects. The following conclusions can be made:

- A 0° cutting has been marked by delamination and bending. With the fiber orientation increase, fiber compression and shearing have been noticed. Cutting at the negative orientation has shown significant fiber bending which complicates cutting mechanisms.
- Surface quality deteriorates with fiber orientation increasing. $\theta = 90^\circ$ is a critical angle, beyond which a severe damage will occur on the surface and the sub-surface.
- A strong correlation has been shown between the fiber behavior during the tool feed and the cutting force and thrust force evolutions. Moreover, friction between the composite (machined surface and chip) and the tool determinates the temperature field cartographies.

As a perspective, various drill geometries will be studied in order to assess its influence on the cutting mechanisms of carbon/epoxy composites.

Acknowledgments Sincere thanks are extended to the Picardie Region for their financial support, to the staff of the Technology Platform of Saint Quentin for their help in the achievement of orthogonal cutting tests, to the staff of the Technical Center for Mechanical Industry CETIM for the analysis of the composite by tomography, and to the staff of the University of Technology of Compiègne for their help in the composite manufacturing.

References

- Li N, Li Y, Zhou J, He Y, Hao X (2015) Drilling delamination and thermal damage of carbon nanotube/carbon fiber reinforced epoxy composites processed by microwave curing. *Int J Mach Tool Manu* 97:11–17
- Gaugel S, Sripathy P, Haeger A, Meinhard D, Bernthaler T, Lissek F, Kaufeld M, Knoblauch V, Schneider G (2016) A comparative study on tool wear and laminate damage in drilling of carbon fiber reinforced polymers (CFRP). *Compos Struct*. doi:10.1016/j.compstruct.2016.08.004
- Duraõ LMP, Tavares JMRS, de Albuquerque VHC, Gonçalves DJS (2013) Damage evaluation of drilled carbon/epoxy laminates based on area assessment methods. *Compos Struct* 96:576–583
- Grilo TJ, Silva RMF, Davim JP (2013) Experimental delamination analyses of CFRPs using different drill geometries. *Compos Part B-ENG* 45:1344–1350
- Turki Y, Habak M, Velasco R, Laurent JN, Vantomme P (2013) An experimental study of drilling parameters effect on composite carbon/epoxy damage. *Key Eng Mat* 554-557:2038–2046
- Babu J, Philip J, Zacharia T, Davim J (2015) Delamination in composite materials: measurement, assessment and prediction. In: Davim JP. *Machinability of fiber reinforced plastics*, Berlin: De Gruyter: 139–162
- Babu J, Sunny T, Paul N, Mohan K, Philip J, Davim J (2015) Assessment of delamination in composite materials: a review. *Proceedings of the Institution of Mechanical Engineers, Part B: Journal of Engineering Manufacture*
- Persson E, Eriksson I, Zackrisson L (1997) Effects of hole machining defects on strength and fatigue life of composite laminates. *Compos Part A-Appl S* 28:141–151
- Duraõ LMP, Gonçalves DJS, Tavares JMRS et al (2010) Drilling tool geometry evaluation for reinforced composite laminates. *Compos Struct* 92:1545–1550
- Wang C, Cheng K, Rakowski R, Greenwood D, Wale J (2016) Comparative studies on the effect of pilot drillings with application to high-speed drilling of carbon fibre reinforced plastic (CFRP) composites. *Int J Adv Manuf Tech*. doi:10.1007/s00170-016-9268-y
- Tsao CC (2008) Experimental study of drilling composite materials with step-core drill. *Mater and design* 29:1740–1744
- Marques AT, Duraõ LMP, Magalhães AG et al (2009) Delamination analysis of carbon fibre reinforced laminates: evaluation of a special step drill. *Compos Sci and Technol* 69:2376–2382
- Zitoun R, Krishnaraj V, Almabouacif BS et al (2012) Influence of machining parameters and new nano-coated tool on drilling performance of CFRP/Aluminium sandwich. *Compos Part B-ENG* 43: 1480–1488
- Rahme P, Landon Y, Lachaud F, Piquet R, Lagarrigue P (2014) Drilling of thick composite material with a small-diameter twist drill. *Int J Adv Manuf Tech*. doi:10.1007/s00170-014-6374-6
- Bonnet C (2010) Comprehensive study of cutting phenomena for titanium alloys Ti6Al4V and CFRP stacks drilling in dry condition (Compréhension des mécanismes de coupe lors du perçage à sec de l'empilage Ti6Al4V/Composite fibre de carbone). Dissertation, ENAM
- Hocheng H, Dharan CKH (1990) Delamination during drilling in composite laminates. *J Manuf Sci E* 112(3):236–239
- Lachaud F, Piquet R, Collombet F, Surcin L (2001) Drilling of composite structures. *Compos Struct* 52:511–516
- Rahmé P, Landon Y, Lachaud F et al (2011) Analytical models of composite material drilling. *Int J Adv Manuf Tech* 52:609–617
- Sedláček J, Humár A (2008) Analysis of fracture mechanisms and surface quality in drilling of composite materials. *Strength Mater* 40(1):48–51
- Seif MA, Khashaba UA, Rojas-Oviedo R (2007) Measuring delamination in carbon/epoxy composites using a shadow moiré laser based imaging technique. *Compos Struct* 79:113–118
- Davim JP, Rubio JC, Abrao AM (2007) A novel approach based on digital image analysis to evaluate the delamination factor after drilling composite laminates. *Compos Sci and Technol* 67:1939–1945
- Duraõ LMP, Magalhães AG, Tavares JMRS, Marques AT (2006) Analyzing objects in images for estimating the delamination influence on load carrying capacity of composite laminates. In: *Proceedings of Composite Image*. Coimbra, Portugal, Taylor & Francis, pp 169–174. ISBN: 9780415433495
- Iliescu D, Gehin D, Iordanoff I et al (2010) A discrete element method for the simulation of CFRP cutting. *Compos Sci and Technol* 70:73–80
- Lin SC, Chen IK (1996) Drilling carbon fiber-reinforced composite material at high speed. *Wear* 194:156–162
- Brinksmeier E, Janssen R (2002) Drilling of multi-layer composite materials consisting of carbon fiber reinforced plastics (CFRP), titanium and aluminum alloys. *CIRP Ann Manuf Technol* 51(1): 87–90
- Merino-Pérez JL, Royer R, Merson E, Lockwood A, Ayvar-Soberanis S, Marshall MB (2016) Influence of workpiece constituents and cutting speed on the cutting forces developed in the conventional drilling of CFRP composites. *Compos Struct* 140: 621–629
- Bonnet C, Poulachon G, Rech J, Girard Y, Costes JP (2015) CFRP drilling: fundamental study of local feed force and consequences on hole exit damage. *Int J Mach Tool Manu* 94:57–64
- Li MJ, Soo SL, Aspinwall DK, Pearson D, Leahy W (2014) Influence of lay-up configuration and feed rate on surface integrity when drilling carbon fibre reinforced plastic (CFRP) composites. *Procedia CIRP* 13. 2nd CIRP Conference on Surface Integrity (CSI): 399–404
- Duraõ LMP, de Moura MFSF, Marques AT (2008) Numerical prediction of delamination onset in carbon/epoxy composites drilling. *Eng Fract Mech* 75(9):2767–2778
- Hintze W, Hartmann D, Schütte C (2011) Occurrence and propagation of delamination during the machining of carbon fibre reinforced plastics (CFRPs)—an experimental study. *Compos Sci and Technol* 71:1719–1726
- Ramirez C, Poulachon G, Rossi F, M'Saoubi R (2014) Tool wear monitoring and hole surface quality during CFRP drilling. 2nd CIRP Conference on Surface Integrity (CSI), *Procedia CIRP*: 163–168
- Poulachon G, Outeiro J, Ramirez C, André V, Abrivard G (2016) Hole surface topography and tool wear in CFRP drilling. 3rd CIRP Conference on Surface Integrity (CIRP CSI) *Procedia CIRP* 45: 35–38
- Gohorianu G (2008) Interaction between drilling defects and bearing behaviour of carbon/epoxy bolted joints (Interaction entre les

- défauts d'usinage et la tenue en matage d'assemblages boulonnées en carbone/époxy). Dissertation, University of Toulouse
34. Krishnaraj V, Prabukarthi A, Ramanathan A et al (2012) Optimization of machining parameters at high speed drilling of carbon fiber reinforced plastic (CFRP) laminates. *Compos Part B-ENG* 43:1791–1799
 35. Arola D, Ramulu M, Wang DH (1996) Chip formation in orthogonal trimming of graphite/epoxy composite. *Compos Part A-Appl S* 27:121–133
 36. Teti R, Machining of composite materials. University of Naples Federico II, Italy
 37. Klocke F, König W, Rummenholler S, Wurtz C (1999) Milling of advanced composites, In *Machining of ceramics and composites*. Eds. Jahanmir S, Ramulu M, Koshy P, Dekker M. Inc.:249–265
 38. Wang XM, Zhang LC (2003) An experimental investigation into the orthogonal cutting of unidirectional fibre reinforced plastics. *Int J Mach Tool Manu* 43:1015–1022
 39. Calzada KA, Kapoor SG, De Vor RE et al (2012) Modeling and interpretation of fiber orientation-based failure mechanisms in machining of carbon fiber-reinforced polymer composites. *J Manuf Process* 14:141–149
 40. Henerichs M, Voß R, Kuster F, Wegener K (2014) Machining of carbon fiber reinforced plastics: influence of tool geometry and fiber orientation on the machining forces. *CIRP J Manu Sci and Tech*. doi:10.1016/j.cirpj.2014.11.002
 41. Bhatnagar N, Ramakrishnan N, Naik NK, Komanduri R (1995) On the machining of fiber reinforced plastic (FRP) composite laminates. *Int J Mach Tool Manu* 35(5):701–716
 42. Venu Gopala Rao G, Mahajan P, Bhatnagar N (2007) Micro-mechanical modeling of machining of FRP composites: cutting force analysis. *Compos Sci and Technol* 67:579–593
 43. Wang DH, Ramulu M, Arola D (1995) Orthogonal cutting mechanisms of graphite/epoxy composite. Part I: unidirectional laminate. *Int J Mach Tool Manu* 35(12):1623–1638
 44. Nayak D, Singh I, Bhatnagar N, Mahajan P (2005) Finite element analysis of effect of machining direction on fibre orientation of FRP composites. *IE(I) Journal-PR* 85:64–67
 45. Santo L, Caprino G, De Iorio I (1998) Cutting forces and cut quality in orthogonal cutting of unidirectional carbon fibre reinforced plastics. *Integrated Design and Process Technology* 3:282–287
 46. Venu Gopala Rao G, Mahajan P, Bhatnagar N (2008) Three-dimensional macro-mechanical finite element model for machining of unidirectional-fiber reinforced polymer composites. *Mater Sci and Eng* 498A:142–149
 47. Iliescu D (2008) Experimental and numerical approaches of machining of dry carbon/epoxy composites (Approches expérimentale et numérique de l'usinage à sec des composites carbone/époxy). Dissertation, ENSAM
 48. Gaitonde VN, Karnik SR, Campos Rubio J et al (2008) Analysis of parametric influence on delamination in high-speed drilling of carbon fiber reinforced plastic composites. *J Mater process tech* 203: 431–438
 49. Biermann D, Feldhoff M (2012) Abrasive points for drill grinding of carbon fibre reinforced thermoset. *CIRP Ann Manuf Technol* 61: 299–302
 50. Tsao CC, Hocheng H (2005) Computerized tomography and C-scan for measuring delamination in the drilling of composite materials using various drills. *Int J Mach Tool Manu* 45:1282–1287
 51. Turki Y, Habak M, Velasco R, Aboura Z, Khellil K, Vantomme P (2014) Experimental investigation of drilling damage and stitching effects on the mechanical behavior of carbon/epoxy composites. *Int J Mach Tools Manuf* 87:61–72